LLNL-TR-741288

LAWRENCE LIVERMORE NATIONAL LABORATORY

Initial Computational Study of a New Multi-Hole Hohlraum (the "Midraum")

M. Tabak, O. S. Jones

November 7, 2017

Disclaimer

This work performed under the auspices of the U.S. Department of Energy by Lawrence Livermore National Laboratory under Contract DE-AC52-07NA27344.

Initial Computational Study of a New Multi-Hole Hohlraum (the "Midraum")

M. Tabak
O. Jones

I. Introduction

Existing cylindrical hohlraums with two oppositely positioned laser entrance holes (LEHs) have multiple constraints. Their goal is to produce radiation sources distributed over the sky, as visible from the spherical implosion capsule, with most of the deposition near the zeroes of the fourth Legendre polynomial in cosine of the polar angle. This requires some of the laser light to propagate across the hohlraum to positions near the hohlraum symmetry plane. The ratio of case spherical radius to capsule spherical radius should exceed 3 so that the light doesn't pass through over-dense ablator plasma. Radiation transport can smooth higher radiation modes. For capsules that demand long pulse lengths, hohlraum walls can blow in and change the position where light is absorbed. This changes the radiation symmetry in a time dependent fashion. This affects both P2 and P4. This wall motion can be reduced by introducing fill gas into the hohlraum. The gas provides back pressure and tamps the wall motion.

Adding the fill gas comes at some cost. It leads to increased absorption of laser light along the path. The fill gas adds heat capacity to the system, ultimately requiring more laser energy to meet the radiation flux goals, both in total and particularly in the amount of radiation coming from the vicinity of the capsule waist. Given the existing beam pointing at NIF energy from the outer beams must be transferred into the inner beams. Cross beam energy transport (CBET) is accomplished via a plasma instability. This transfer is not perfectly predictable. In addition, the higher intensity required to make up for the losses along the long path can lead to stimulated backscatter as well as the generation of suprathermal electrons.

The inner beams will pass through the plasma ablated from the capsule toward the end of the pulse. Heating this plasma acts as another parasitic loss. In addition, the light passing through the turbulent blow-off can be refracted in unpredictable directions.

II. What we propose

We propose to alter the shape of a standard cylindrical hohlraum to allow the NIF beams with polar angles of 23.5 and 30 degrees (usually referred to as the inner cone beams) to enter the hohlraum through additional LEHs located close to the midplane of the hohlraum. This is accomplished by making the radius of the hohlraum larger at the midplane, and adding 4 small laser entrance holes per side on the section that connects the smaller radii part to the larger radii part. This configuration, which we will refer to as the "midraum", is shown in Figure 1. Note that the path lengths for the inner cone beams are ~2-3 mm, whereas for a standard cylindrical 2-LEH configuration they would be ~ 5-7 mm. This should result in less inverse bremsstrahlung absorption along the beam path and more energy delivered to the wall. Rerouting the beams this way also removes the possibility of CBET between the inner and outer cone beams, which eliminates this potential source of uncertainty.

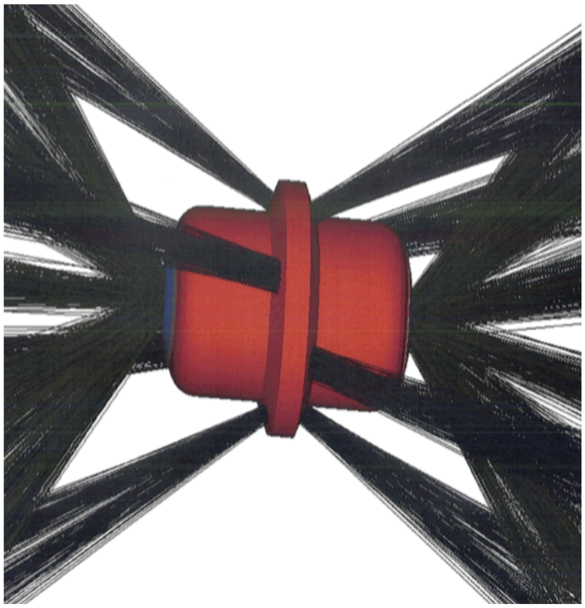

Figure 1 – 3D illustration of the midraum concept.

Figure 2 shows our computational design in two dimensions. The figure shows the right half of a symmetric calculation. The inner cone beams beams are injected into the problem through two annular holes at the midplane that are centered at 2.1 and 2.5 mm radius with rays that run parallel to the axis. In reality, they would enter through an LEH about a mm to the left of the midplane in the figure, but that is not possible with this particular axisymmetric grid configuration. These parallel beams are designed to mock up the 23.5 and 30 degree beams. Separately weighting the power to the 23.5 and 30 degree beams gives some time dependent control of the P4. Since there is no true LEH near the midplane, we allow plasma and radiation to leak out through the annuli and force the annuli to have the same area as 4 circular holes with individual radii of 500 microns. Otherwise, the midplane at z=0 acts as a symmetry plane. This geometry is clearly a simplification of the actual hohlraum geometry, which is 3D in nature. We will develop more accurate models in the future. Eventually, we would like to perform 3D calculations.

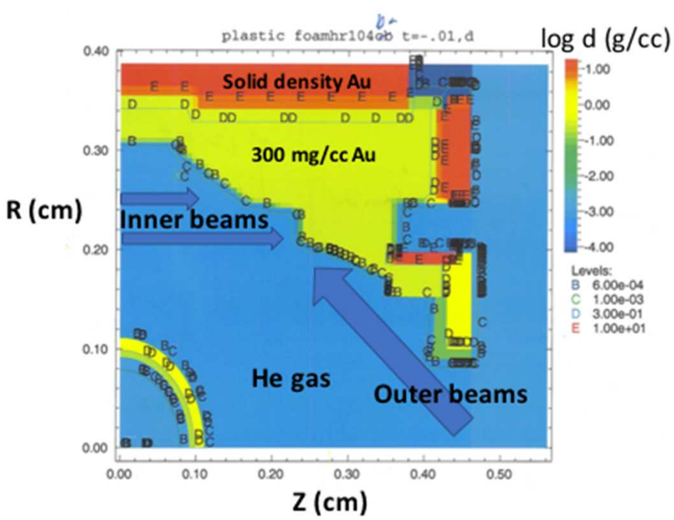

Figure 2 – Axisymmetric calculation of the midraum using foam high Z walls

Hohlraum walls are gold with density 0.3 gm/cc backed by solid gold. The lower wall density reduces the energy loss to hydrodynamic motion. More importantly the lower density walls are more easily tamped by the fill gas. Less wall motion with lower fill gas densities result.

III. Results

We have used the hohlraum shown in Figure 2 to drive 2 different implosion capsules: a capsule with diamond ablator and 9 ns pulse length, and a capsule with CH ablator and a 20-ns drive pulse shape designed to adiabat-shape the ablator. Adiabat shaping, where the ablator is on a high

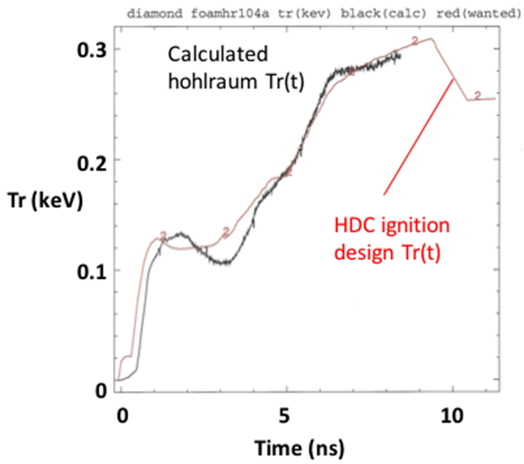

Figure 3 – HDC ignition design radiation drive (red) and radiation temperature extracted from midraum calculation (black).

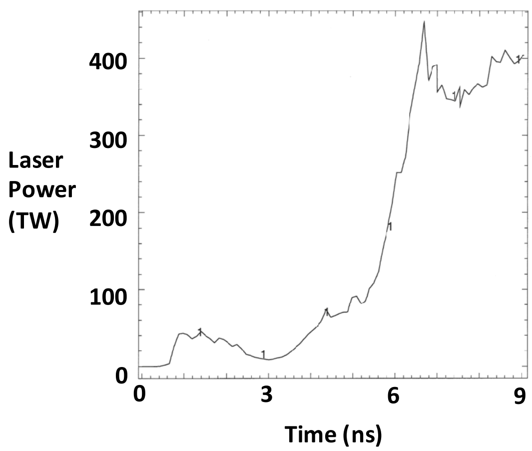

Figure 4 – Calculated absorbed laser power required to match the HDC TR(t) in midraum

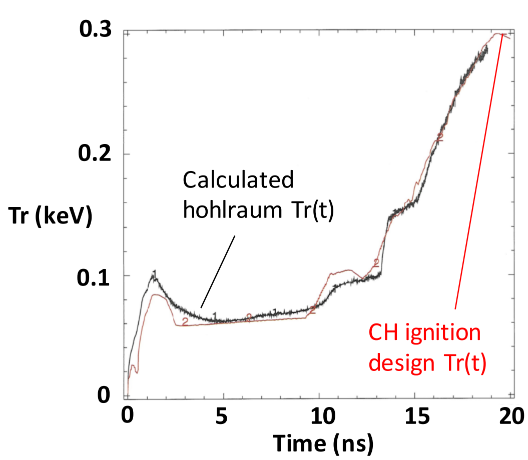

Figure 5 – CH adiabat-shaped design Tr(t) (red) and radiation temperature extracted from midraum calculation (black)

adiabat and the fuel is on a lower adiabat, increases the stability of the ablation while maintaining the high density of the compressed fuel. The diamond capsule has 40% more mass than the plastic capsule. Both of these time-dependent radiation drives are designed to drive an ignition capsule with a DT ice layer.

The HDC capsule has an outer radius of 1108 microns, an ablator thickness of 76 microns, and a DT fuel thickness of 56 microns. The HDC ablator is doped with 0.275% tungsten dopant. This is a high gain design. The capsule absorbs about 150 kJ of energy and the calculated 1D yield is > 16 MJ. Figure 3 shows the desired radiation pulse shape for the diamond capsule together with the calculated radiation temperature history out to ~8 ns. The average radiation temperature plotted is the fourth root of the flux across a surface at radius 1.5 mm. Figure 4 shows that this hohlraum requires a peak absorbed laser power of ~400 TW to achieve the desire peak drive temperature. If this calculation were continued about another ns to the end of the laser pulse, it would require ~1.7 MJ in absorbed laser energy.

The CH capsule has an outer radius of 1111 microns, an ablator thickness of 193 microns, and a DT fuel thickness of 70 microns. This is not a high gain design. The capsule absorbs ~ 100 kJ of energy and gives ~ 1 MJ of yield in 1D. Figure 5 shows the radiation drive for the adiabat shaped pulse for the CH capsule. The peak drive temperature also reaches 300 eV as in the HDC case, but the integral of Tr^4 while the laser is on (drive rising) is ~30% less in the CH case. Figure 6 shows that the required laser peak power is < 400 TW at 19 ns, when this particular calculation stopped. If the calculation were continued to the end of the laser pulse, the projected required absorbed laser energy would be 1.2 MJ, or about 40% less than for the high gain HDC design. These energy estimates assume there is no laser reflection due to plasma instabilities and that our hohlraum model is correct.

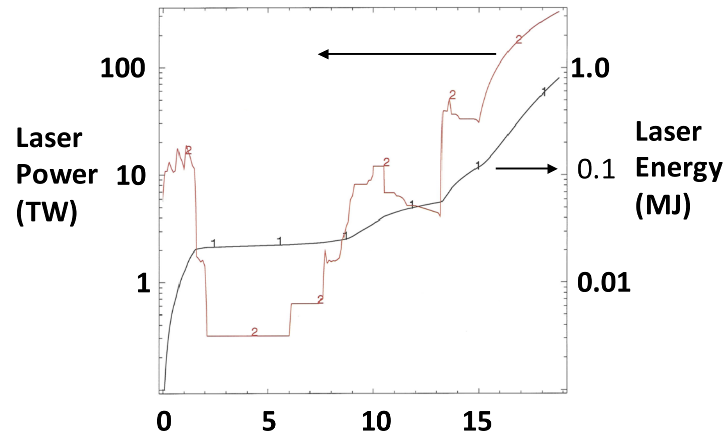

Figure 6 – Laser power and energy required to produce the Tr(t) for the adiabat-shaped CH design

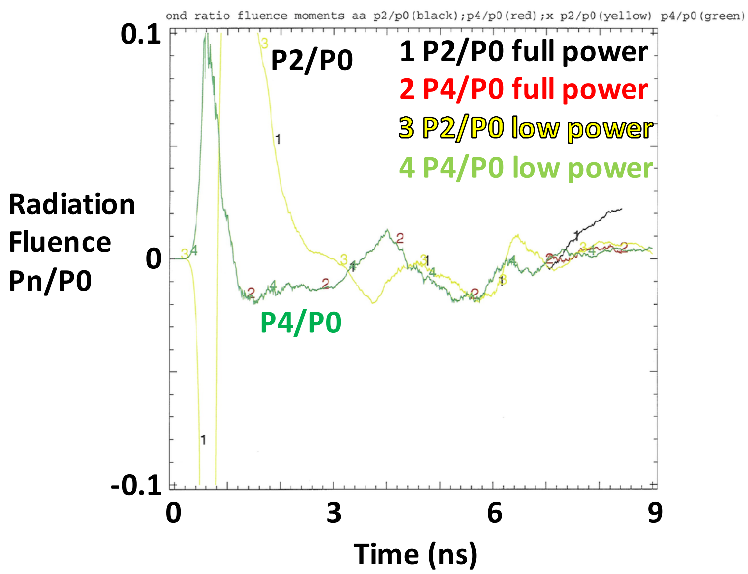

Figure 7 – Legendre moments of the radiation flux at r=0.15 cm for the HDC calculation.

These calculations should be less sensitive to electron conductivity than the conventional cylindrical 2-LEH hohlraum designs because in the midraum the inner beam light is absorbed in the same material that radiates x-rays. In the conventional cylindrical hohlraums, inner beam light propagating toward the waist is absorbed in low atomic number plasma which must then conduct energy to the high atomic number wall before the energy can produce x-rays. This should make the radiation symmetry more predictable for the midraum. Figure 7 shows the P2 and P4 Legendre moments of the incoming radiation fluence at radius of 0.15 cm for the HDC calculation. Ideally, we would like the P2 and P4 fluence moments to be close to zero at the end of the drive. Two cases are plotted. Curves 3 and 4 are the P2/P0 and P4/P0 fluence moments for the case where the peak power is reduced after 6.5 ns. In this case (which has a peak Tr of 280 eV), both P2/P0 and P4/P0 are < 1%. Curves 1 and 2 are the P2/P0 and P4/P0 fluence moments for the full power case (the laser power shown in Figure 4, which produces 300 eV). After 7 ns the drive becomes pole high as the density along the inner beam path increases and the more energy is absorbed farther from the wall, so the integrated P2/P0 is > 2%. This can be remedied by increasing the laser flux through LEH's over the hohlraum waist.

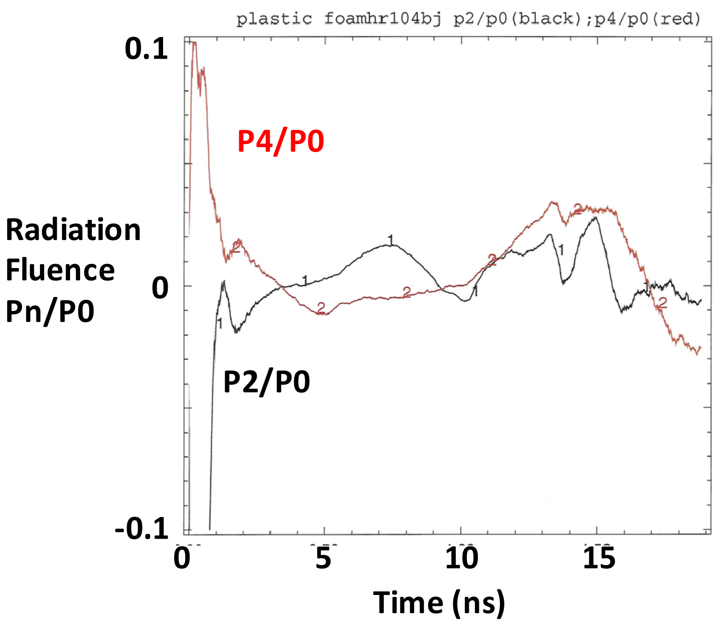

Figure 8 – Legendre moments of the radiation fluence at r=0.15 cm for the adiabat-shaped CH calculation.

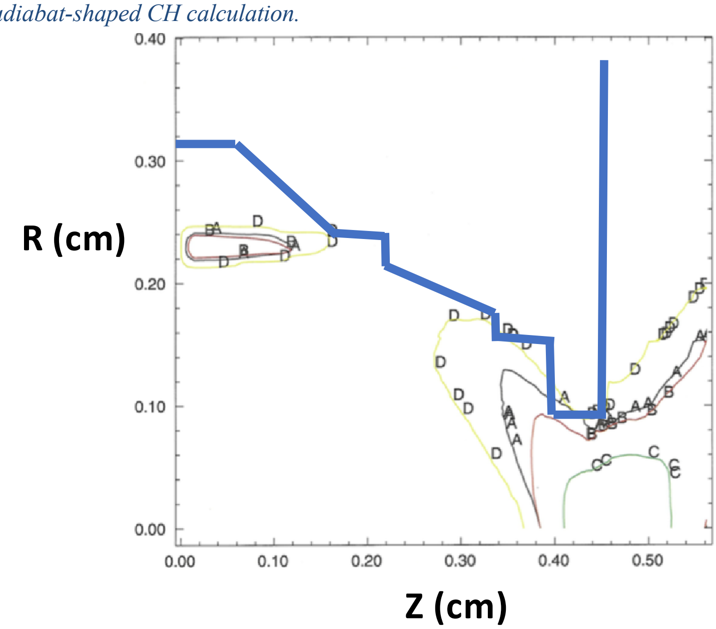

Figure 9 – Contours of 10^{14} W/cm^2 at 10.5 ns (C), 14 ns (A), 15 ns (B), and 18.8 ns (D).

Figure 8 shows similar moments for the adiabat-shaped pulse driving the plastic capsule. The P2-moment is well controlled and held below 1%. The P4 moment peaks at 3% at 15 ns. In this geometry, this moment is uncontrolled. This difficulty is a consequence of adiabat shaping. Adiabat-shaping uses an initial decaying shock to heat the outside of the ablator. The decaying shock is launched by an impulsive pressure pulse. That is, high initial pressure is rapidly reduced. In a hohlraum, this requires essentially turning off the laser after a short high-power interval. During this interval, the wall plasma expands and cools. When the laser intensity increases leading to the main pulse, the light is absorbed farther from the original position of the gold. As the plasma heats, the laser can burn through this plasma and be absorbed closer to the wall. Figure 9 shows this variation in penetration. The figure shows the position of the 10^{14} W/cm^2 laser intensity contour at 10.5 ns (contour C), 14 ns (A), 15 ns (B), and 18.8 ns (D). The lasers incident over waist (inners) and the outer beams penetrate less at 15 ns (beginning of main rise) than they do at 18.8 ns (peak power). This time-dependent change in the position of the laser absorption causes a swing in P4/P0 during this time interval. The next version of this design will obtain more dynamic range by moving the wall the inner beams interact with, to the right, and perhaps making the main LEH larger.

The electron density near the outer LEH peaks at about 10% of critical density, while that near the inner LEH's has electron density approaching 18% of the critical density. Laser plasma instabilities may have unacceptably large growth rates at this electron density. This density is high because the expanding plasma flows from the high atomic number wall and the expanding plasma meet here. Possible fixes are to increase the distance from the radiating spots to the capsule by increasing the radius of the hohlraum near this point and to increase the radii of those LEH's in order to increase the flow of material through the holes.

IV. Design of small laser entrance holes

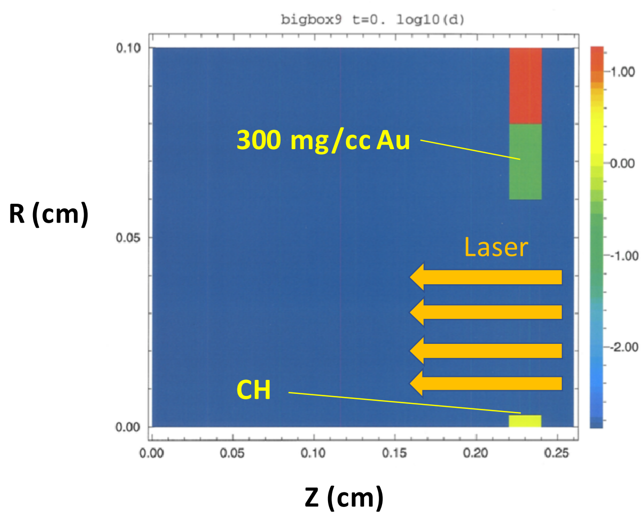

Figure 10 - Calculation of LEH closure for HDC drive with 300 mg/cc Au foam liner and CH wire and Tr source on left boundary.

This hohlraum design requires LEH's substantially smaller than the 1.5 mm radius LEH used in the conventional design because adding 8 LEH's of that radius would cause the radiative losses to be about ten times the energy absorbed by the capsule and reduce the amount available for the capsule below the ignition threshold. Our design for such LEH's use low density wall material (0.3 g/cc Au/U) and employs a novel low atomic number (CH) wire in the center of the LEH.

The idea is to maintain pressure equilibrium between radiative heated LEH wall and the laser heated low-Z material filling the hole. Unfortunately, the low-Z material will escape from the hohlraum faster than the high-Z material will so at some time the wall and the fill are no longer in pressure balance and the hole shuts. We place a plastic wire with density 1.05 g/cc and radius 30-50 microns in the center of the LEH. The wire ablates in time supplying enough material to keep the hole open. This technique differs from the more conventional one of lining the LEH with plastic, because a plastic liner of thickness of, say, one micron would burn through very quickly and not be available late in time. A thick liner whose burn through time was comparable to the

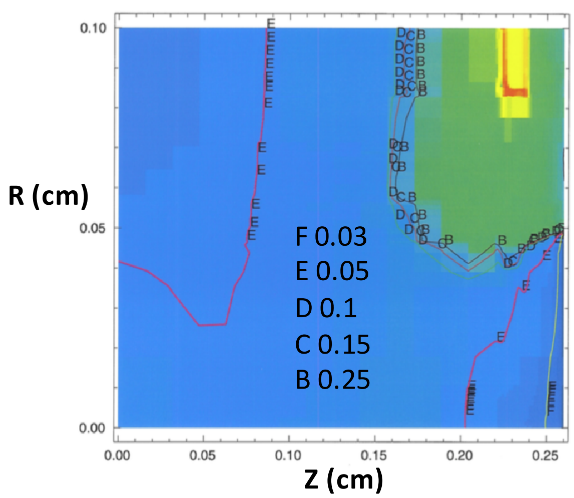

Figure 11 – Contours of n_e/n_c for HDC drive at 9 ns (end of peak power).

capsule implosion time would supply too much plasma and result in laser-plasma instabilities or in an over dense plasma blocking the LEH.

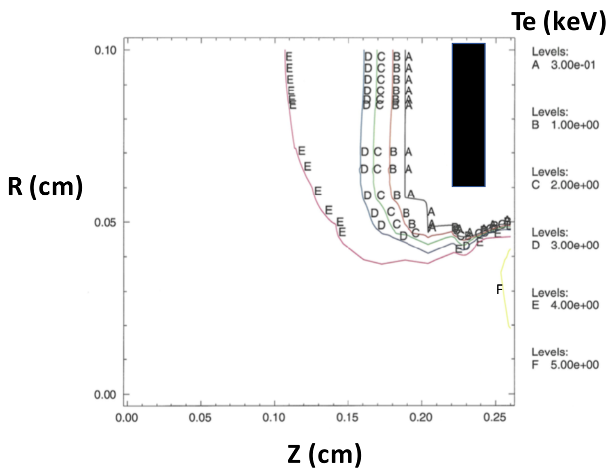

Figure 12 – T_e contours for HDC drive at 9 ns.

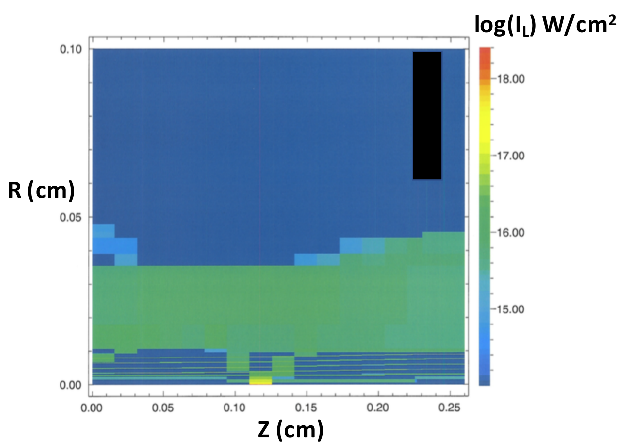

Figure 13 – Contours of laser intensity for HDC drive at 9 ns.

Figure 10 shows such an LEH design where the laser light enters from the right through the LEH and is allowed to propagate out of the computational volume at the left boundary. The laser light power is that required for one small midplane LEH driving the HDC capsule (400 TW / 24 because 2 quads go through each midplane LEH) and a radiation temperature source is supplied at the back surface given by the temporal history of the temperature driving the HDC capsule (see Figure 3). Matter is allowed to flow out only through the LEH. Figure 11 shows the electron density at 9 ns, the end of the pulse; Figure 12 shows the electron temperature at 9 ns; Figure 13 shows the laser intensity at 9 ns (the rays have 0 spreading angle). In this case the LEH radius is 600 microns and the laser spot radius is 400 microns. Assuming a peak power of 400 TW and that each quad has the same peak power, the average overlapped intensity in the heated portion of the LEH is ~ 3e15 W/cm^2. However, Figure 13 shows that the local intensity is closer to 1e16 W/cm^2, probably due to self-focusing. Of the incident 116 kJ of light entering the LEH, 106 kJ escape out the back and 14 kJ of radiation escapes through the LEH. In this simple mode of the LEH, most of the laser light gets into the hohlraum. The peak electron temperature is ~ 5 keV, and the electron density remains about 5% of critical. Because there is no hohlraum wall, this model underestimates the hohlraum filling.

Figure 14 is similar to figure 10, but here we put a density 0.3 g/cc au/u material at the back surface to intercept the incident laser light and to act as a model for the radiating region used in the integrated hohlraum design. Figure 15, which is a contour plot of the electron density relative to the critical density at 8 ns, shows that the LEH stays open and peak electron density in the laser path is less than 0.1 critical density. The volume does fill with high-Z material, but the light still propagates. Figure 16 shows the electron temperature distribution at this time. Future designs will extend the wire on axis to

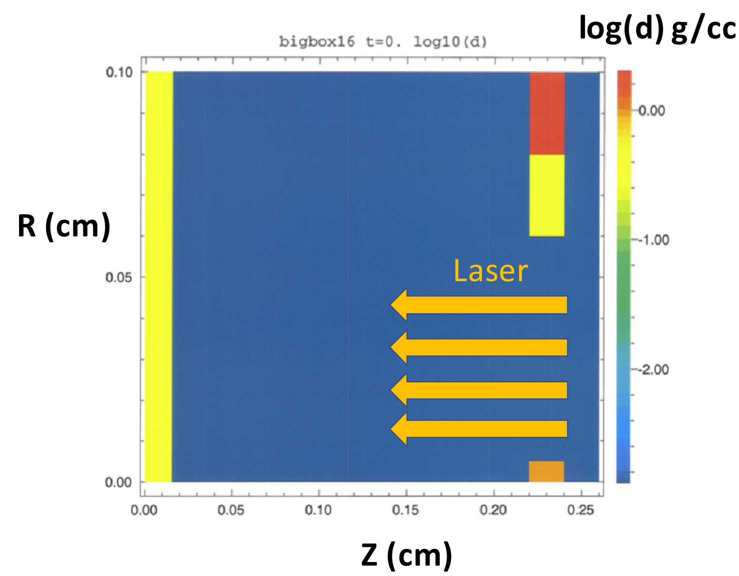

Figure 14 – Calculation of LEH closure for HDC drive with foam gold boundary on left included.

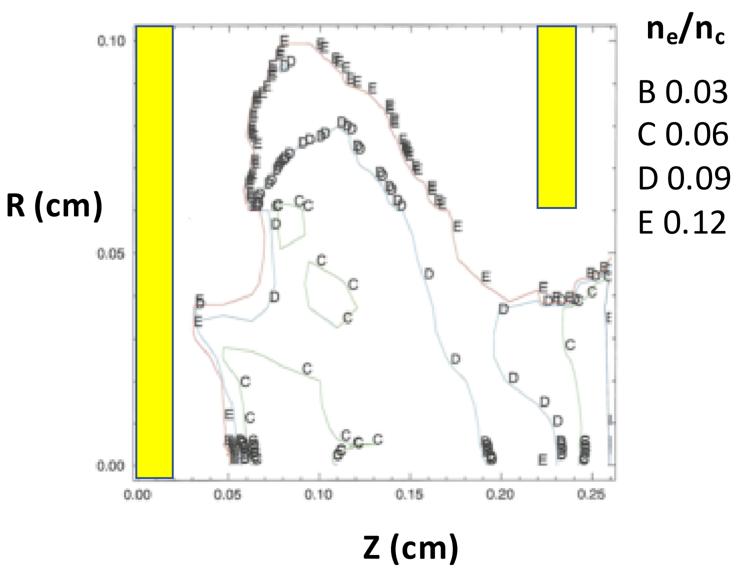

Figure 15 – Contours of n_e/n_c for HDC drive at 8 ns with foam Au on left boundary.

increase the volume where low-Z substitutes for high Z. The radiation escaping through the LEH varies between 1/10 and 1/6 of the incident laser light. This is comparable to the radiation losses from conventional hohlraums.

The integrated design calculations shown above (Figure 2, etc.) had peak laser intensity near the symmetry plane above 2e15 W/cm^2. This intensity is high enough to have considerable risk for exciting damaging laser-plasma-interactions. In the real 3D case, the overlapped beam intensity will be higher because the beam is not annular as in the axisymmetric calculation, but has a circular spot and enters through a circular LEH. Figure 17 shows the laser intensity at 8 ns in the LEH-only calculation (e.g. Figure 14). The overlapped intensity in the LEH for a mixture of beams with opening angles 0,15 and 30 degrees, respectively, approaches 1e16 W/cm^2 in the LEH, but drops quickly with distance. The overlapped beam intensity should be comparable to that in the conventional designs. But because the midplane LEH's have smaller radii to minimize LEH losses, the beam radii should be reduced by a factor of two. So, the single beam intensities might increase by a factor of 4. Fortunately, individual beamlets can be sent to different LEH's. Then the relevant intensity should be the single beamlet intensity. We are left with the intensity to be considered for LPI calculations between 1-2 times that of conventional hohlraums.

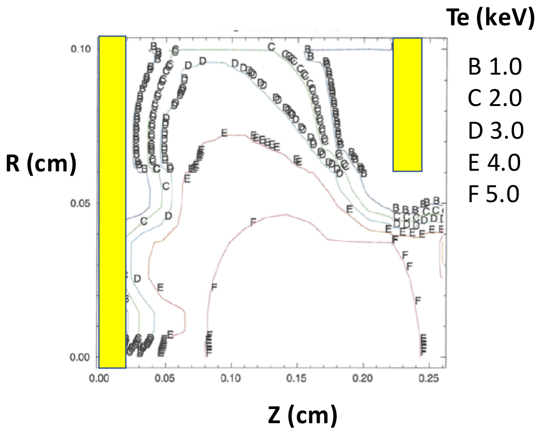

Figure 16 – Contours of Te for HDC drive at 8 ns with foam Au on left boundary.

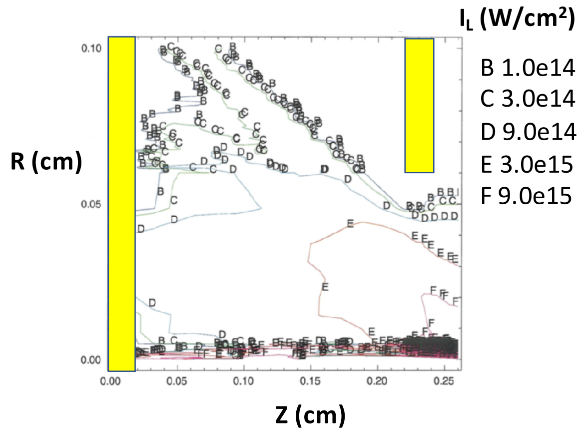

Figure 17 – Contours of laser intensity for HDC drive at 8 ns with foam Au on left boundary.

This small LEH design, if successful, can have applications broader than just this hohlraum design. If applied to the conventional hohlraum, it would reduce losses by about 100 kJ while reducing a major source of radiation asymmetry. If the design can be pushed to small holes, it enables a spherical hohlraum design with many small holes, small shadows and static radiation symmetry.

V. Summary

We have shown initial designs for hohlraums with additional LEH's placed near the target equator. The design allows independent delivery of energy to the inner and outer radiation sources driving the capsule. The path-lengths of light through plasma are significantly shortened, but laser intensities are increased. The hohlraum driving a capsule with diamond ablator can deliver adequate P2 and P4 radiation symmetry moments. The hohlraum driving the adiabat-shaped capsule with plastic ablator has adequate P2 symmetry, but a 3% excursion when the laser power begins to rise after low power part of the pulse. Descriptions of possible paths to remedy these problems have been suggested. Designs of small LEH's have been described. These are required for this scheme to be viable and may improve or enable other hohlraum schemes as well.

Acknowledgements

This work was performed under the auspices of the U.S. Department of Energy by Lawrence Livermore National Laboratory under contract DE-AC52-07NA27344. This work was funded by Laboratory Directed Research and Development (LDRD) project 15-ERD-058.